

Enhanced disturbance suppression in sampled-data systems and its application to high density data storage servos

Chee Khiang Pang · Guoxiao Guo · Ben M. Chen ·
Tong Heng Lee

Received: 27 June 2006 / Accepted: 13 October 2006 / Published online: 16 November 2006
© Springer-Verlag 2006

Abstract Precise servo control systems require strong disturbance rejection capabilities for accurate positioning in the nanometer scale world today. In this paper, we propose an add-on DDO (disturbance decoupling observer) and DDOS (DO with extraneous sensor) for stronger disturbance suppression. Our proposed control methodology uses a nominal plant model and its inverse to reject input and output disturbances simultaneously in sampled-data systems. The plant inverse controller is approximated by tuning a single parameter ε . Experimental results on a PZT actuated servo system with air flow of mean speed of 50 m/s corresponding to 15,000 rpm in today's high end hard disk drives show an improvement of 69.2% of 3σ PES (position error signal) during track-following.

1 Introduction

Reduction of \mathcal{H}_2 - and \mathcal{H}_∞ -norms from disturbance sources to controlled output remain an important measure of designing servo systems for precision servo systems. These demands of ultra high and precise servo positioning accuracy directly translate into a high

bandwidth servo system for ultra strong disturbance and vibration rejection capabilities. While the disturbance sources can be generally classified as periodic and aperiodic, most current disturbance rejections schemes are concerned with tackling them independently. Interested readers are referred to works by Duan (2005) for feedforward periodic RRO (repeatable run-out) compensation and Pang et al. (2005a) for online iterative control of aperiodic NRRO (non-repeatable run-out) rejection in HDDs.

To tackle the disturbance sources simultaneously, the effects of disturbances should be cancelled before they affect the true controlled output. This effectively requires making the sensitivity transfer function matrix S or \mathcal{H}_2 - and \mathcal{H}_∞ -norms from output disturbance sources to controlled output to zero, the latter being commonly known as DDPs (disturbance decoupling problems). Several disturbance decoupling (setting the norms to zero) and almost disturbance decoupling (almost zero) schemes have been proposed. Lin et al. (2000) explicitly parameterized in a single parameter which solves the well-known \mathcal{H}_∞ -ADDPMS (\mathcal{H}_∞ -Almost DDP with measurement feedback and with internal stability) for discrete-time linear systems. Chen et al. (1999) extended the framework and applied to disturbance decoupling control of a piezoelectric bimorph actuator with hysteresis successfully.

Alternatively, improved disturbance rejection capabilities via the construction of disturbance observers have also been introduced by Ohnishi (1987). White et al. (2000) constructed a disturbance observer for improved track-following capabilities in HDDs without additional sensors. Goodwin (2000) also showed that introduction of these schemes are highly cost effective and attractive alternatives to

C. K. Pang (✉) · G. Guo
A*STAR Data Storage Institute,
No. 5, Engineering Drive 1,
Singapore, Singapore 117608
e-mail: ckpang@nus.edu.sg

C. K. Pang · B. M. Chen · T. H. Lee
Department of Electrical and Computer Engineering,
National University of Singapore, Singapore, Singapore

embedding sensors which are susceptible to measurement noise.

In this paper, an add-on DDO (disturbance decoupling observer) and DDOS (disturbance decoupling observer with extraneous sensor) into current sampled-data systems to mimic disturbance decoupling effects are proposed. The proposed DDO uses the identified discretized plant model and its inverse to reject input disturbances and output disturbances simultaneously. The nominal plant inverse is obtained by tuning a single parameter ε to approximate the causality of the improper plant inverse. The proposed control methodology is evaluated with simulation and experimental results on a PZT actuated passive suspension mounted on a head cartridge for usage on a spindrive as reported by Wong et al. (2005).

The rest of the paper is organized as follows. Section 2 introduces the proposed add-on DDO to the nominal digital controller in sampled-data systems for stronger disturbance rejection capabilities. In Sect. 3, the DDO is extended to DDOS with extra information from embedded sensors for enhanced disturbance attenuation. Section 4 describes an industrial application of the proposed DDO on a PZT actuated passive suspension with air flow mimicking input and output disturbances in current 2.5" high end HDDs. Conclusion with future work directions are summarized and discussed in Sect. 5.

2 Disturbance decoupling observer

For simplicity but without loss of generality, consider the following SISO (single-input–single-output) digital sampled-data servo control system regulation problem with proposed DDO as shown in Fig. 1.

The control signal u is given by

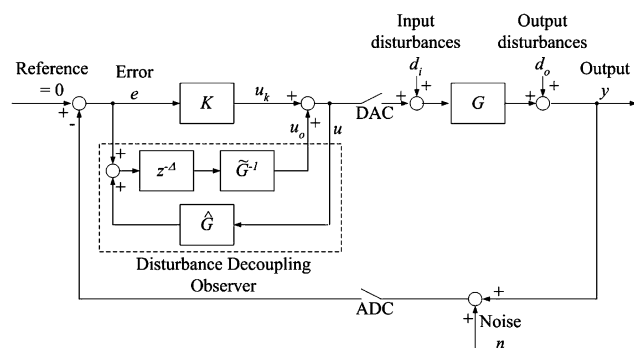


Fig. 1 Block diagram of servo sampled-data control system with proposed DDO

$$\begin{aligned}
 u &= u_k + u_o \\
 &= Ke + z^{-\Delta} \tilde{G}^{-1} \hat{G}u + z^{-\Delta} \tilde{G}^{-1} e
 \end{aligned}
 \tag{1}$$

where \hat{G} is the identified discretized mathematical model of the plant to be controlled $G(s)$ using a ZOH (zero order hold) equivalence at a chosen sampling rate the stable pole-zero pairs of plant $G(s)$ remain in the unit disc using the guidelines depicted by Åström et al. (1984). Δ is an integer included to prevent computational singularity and its choice will be detailed in future sections. \tilde{G}^{-1} is the proper and minimum phase inverse of the \hat{G} . The procedure to obtain \tilde{G}^{-1} will be proposed in the next subsection.

Straight forward manipulation results in

$$\begin{aligned}
 y &= d_o + Gd_i + Gu \\
 &= \frac{1 - z^{-\Delta} \tilde{G}^{-1} \hat{G}}{1 - z^{-\Delta} \tilde{G}^{-1} \hat{G} + GK + z^{-\Delta} \tilde{G}^{-1} G} (d_o + Gd_i) \cdots \\
 &\quad - \frac{GK + z^{-\Delta} \tilde{G}^{-1} G}{1 - z^{-\Delta} \tilde{G}^{-1} \hat{G} + GK + z^{-\Delta} \tilde{G}^{-1} G} n
 \end{aligned}
 \tag{2}$$

The main motivation of the proposed DDO comes from the renowned IMP (internal model principle) which includes \hat{G} as part of the feedback controller for state estimation. \tilde{G}^{-1} compensates the resonant poles of the plant and also decreases its relative degree for lower sensitivity.

The results can be expanded to MIMO (multi-input–multi-output) framework if G is square and non-singular.

2.1 Complete disturbance suppression

In view of Eq. 2, we propose the following

Theorem 1 Consider the following optimization problem

$$V = \arg \min_{\mu} \left\| 1 - z^{-\Delta} \tilde{G}^{-1}(\mu) \hat{G} \right\|_{\infty}
 \tag{3}$$

subject to $\Delta = 0$ and the constraint

$$\tilde{G}^{-1}(\mu) \in R\mathcal{H}_{\infty}
 \tag{4}$$

we can obtain perfect disturbance suppression with proposed DDO if the plant G is proper and of minimum phase.

Proof 1 Assuming a chosen sampling frequency f_s such that the pole-zero pairs of stable plant G remain in the unit disc (Åström et al. 1984) and non-minimum phase behaviour of the plant is removed. The ZOH

discrete equivalence of plant G with model \hat{G} can be written in standard state-space formulation as

$$x(k + 1) = \Phi x(k) + \Gamma u(k) \tag{5}$$

$$y(k) = Hx(k) + Ju(k) \tag{6}$$

where $\Phi, \Gamma, H,$ and J are the sampled-data system state matrix quadruple.

The plant inverse model \tilde{G}^{-1} can then be obtained via

$$\begin{bmatrix} \Phi & \Gamma \\ H & K \end{bmatrix}^{-1} = \begin{bmatrix} \Phi - \Gamma J^{-1} H & \Gamma J^{-1} \\ -J^{-1} H & J^{-1} \end{bmatrix} \tag{7}$$

From Eq. 2, the first term becomes zero and we have only

$$y = -n \tag{8}$$

which shows that the proposed DDO cancels the input disturbances d_i and output disturbances d_o . Only the effects of measurement and sensor noise permeate to the true controlled output y .

While this method extends only to stable and proper systems (translating to direct feedthrough from control signal u to output y), it is not viable for physical systems which are generally low pass in nature. Moreover due to the constraint of $S + T = 1$ where S is the sensitivity transfer function and T being the complementary sensitivity transfer function, Theorem 1 makes $S = 0$ or an infinite bandwidth servo system which is not achievable in practice.

2.2 Almost disturbance suppression

Most physical systems are strictly proper with high frequency roll-off characteristics in nature. As such if the digital inverse model \tilde{G}^{-1} can only be approximated up to high frequencies—for e.g. using the ZPET (zero phase error tracking) algorithm (Tomizuka 1987) or the NPM (near perfect modelling) methodology (Pang et al. 2005b)—before Nyquist frequency in sampled-data systems to prevent unbounded control signals. The disturbance rejection capabilities of the proposed DDO is deteriorated, with the performance of the servo system now determined by the proximity of the inverse plant model \tilde{G}^{-1} and the true plant inverse \hat{G}^{-1} at most frequencies. The effects of measurement and sensor noise n will also be attenuated by the complementary sensitivity transfer function.

Obviously, $J = 0$ if G is strictly proper as the relative degree of G is now at least one. While Theorem 1 still

holds, Proof 1 does not as singularity now occurs when evaluating J^{-1} in Eq. 7. As such, we propose the following simple methodology using a singular perturbation approach (Kokotović et al. 1986; Lewis et al. 1999; Saberi et al. 1993).

Proposition 1 Consider Theorem 1 and the inverse dynamics problem posed in Eq. 7. The singularity encountered in $J = 0$ is avoided using a singular perturbation technique by first introducing a scalar ε into the state space representation of strictly proper plant G

$$\dot{x} = Ax + Bu \tag{9}$$

$$y = Cx + \varepsilon u \tag{10}$$

where $A, B,$ and C are the system state matrix triple with $0 < \varepsilon \ll 1$. After ZOH discretization, the singular perturbed system is invertible using Eq. 7.

Similarly, we assume a chosen sampling frequency f_s such that the pole-zero pairs of singular perturbed system remain in the unit disc (Åström et al. 1984) and non-minimum phase behaviour of the plant is removed. The proof is now straightforward and ε acts as a controller tuning parameter. If we choose $0 < \varepsilon \ll 1$, the sensitivity transfer function S also approaches zero and we get the following approximation

$$y \approx -n \tag{11}$$

The geometric interpretation $S + T = 1$ is shown in Fig. 2. It is worth noting that using the singular perturbation approach, decreasing ε has the effect of increasing bandwidth of the servo system (better disturbance suppression) and the size of norm of vector T (hence reducing the size of norm of vector S) without decreasing the size of θ where θ is the angle between S and T . A small θ is hence ideal as a large θ causes large peaks in the largest singular values of both S and T .

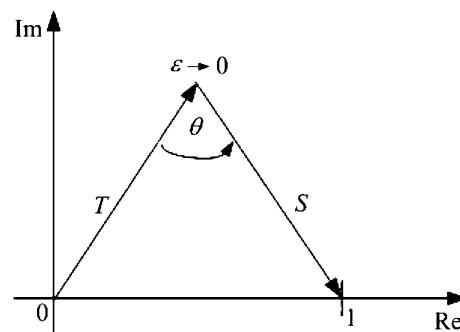


Fig. 2 Geometric interpretation of feedback control constraint $S + T = 1$

2.3 Choice of delay order Δ

However, the proposed singular perturbation method is sensitive to effects of high frequency measurement and sensor noise. In practice, this method of evaluating the plant inverse \tilde{G}^{-1} deteriorates when the relative degree of the plant is large. This is apparent due to the large differentiating effects at high frequencies on attempting plant inversion. As such, the delay element is included to compensate for the relative degree by placing excess deadbeat poles. A rule of thumb for choosing Δ is to set it as the difference between the relative degree and two. The inclusion of the delay term with an appropriate choice of Δ increases θ and also avoids large peaks in S and T .

3 Disturbance decoupling observer with extraneous sensor

Addition of sensors to control systems are known to enhance servo performance and alleviate the observers' orders used in controller designs. In this section, we introduce a DDOS when additional information are available for feedback control with state measurements. This can be obtained via embedding additional sensors or SSA (self-sensing actuation), the latter being more ideal as it requires only cheap electronics while achieving sensor-actuator collocation pair (Pang et al. 2006).

Similarly, consider the following SISO digital sampled-data servo control system regulation problem with proposed DDOS as shown in Fig. 3.

The control signal u is given by

$$u = u_k + u_o = Ke + z^{-\Delta} \tilde{G}^{-1} (\hat{G}u - y - n_2) \tag{12}$$

where n_2 is the noise introduced by the additional sensor. It is assumed that the noise sources n_1 and n_2 are mutually uncorrelated.

Straight forward manipulation again yields the following relation

$$y = d_o + Gd_i + Gu = \frac{1 - z^{-\Delta} \tilde{G}^{-1} \hat{G}}{1 - z^{-\Delta} \tilde{G}^{-1} \hat{G} + GK + z^{-\Delta} \tilde{G}^{-1} G} (d_o + Gd_i) \cdots - \frac{GK}{1 - z^{-\Delta} \tilde{G}^{-1} \hat{G} + GK + z^{-\Delta} \tilde{G}^{-1} G} n_1 \cdots - \frac{z^{-\Delta} \tilde{G}^{-1} G}{1 - z^{-\Delta} \tilde{G}^{-1} \hat{G} + GK + z^{-\Delta} \tilde{G}^{-1} G} n_2 \tag{13}$$

Similarly, the results can be expanded to MIMO framework if G is square and non-singular.

3.1 Complete disturbance suppression with extraneous sensor

With the new results and additional actuator information, we propose the following

Theorem 2 Consider Theorem 1 and the inverse dynamics problem posed in Eq. 7. We can achieve perfect disturbance suppression using the additional sensor and the noise sources n_1 and n_2 are attenuated by T and S , respectively. T and S are the nominal complementary sensitivity and sensitivity transfer functions.

Proof 2 Refer to the control block diagram with proposed DDOS depicted in Fig. 3. By setting $u_o = 0$, the nominal complementary sensitivity transfer function T and sensitivity transfer function S are given by

$$T = \frac{GK}{1 + GK} \tag{14}$$

$$S = \frac{1}{1 + GK} \tag{15}$$

If Theorem 2 is satisfied, then the true controlled output y in Eq. 13 reduces to

$$y = -\frac{GK}{1 + GK} n_1 - \frac{1}{1 + GK} n_2 = -Tn_1 - Sn_2 \tag{16}$$

Dissimilar to the DDO where the noise n permeates to the true controlled output y , the DDOS using an extraneous sensor offers attenuation of nominal noise n_1 with nominal complementary sensitivity transfer function T which is in essence a low pass filter. The noise source n_2 introduced by the additional sensor becomes an output disturbance to the nominal control loop. This implies that additional output information—although the same measurement—can be used to achieve disturbance rejection and noise attenuation simultaneously assuming that noise sources n_1 and n_2 are uncorrelated. As such, the effects of noise on including additional sensor can be removed with any loop shaping design for low sensitivity.

3.2 Almost disturbance suppression with extraneous sensor

Analogous to the almost disturbance suppression in DDO, the almost disturbance suppression with extraneous sensor in DDOS avoids the singularity encoun-

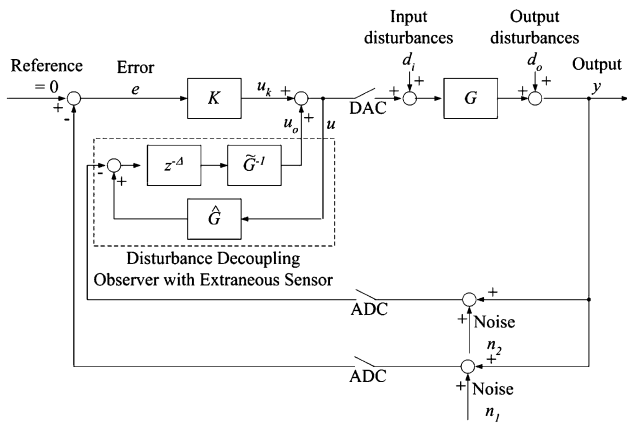


Fig. 3 Block diagram of servo sampled-data control system with proposed DDOS

tered in $J = 0$ for physical systems by using the singular perturbation technique with $0 < \varepsilon \ll 1$ (Kokotović et al. 1986; Lewis et al. 1999; Saberi et al. 1993) as mentioned in the previous section.

Proposition 2 Consider Theorem 1, Theorem 2 and the inverse dynamics problem posed in Eq. 7. The singularity encountered in $J = 0$ is avoided using a singular perturbation technique by first introducing a scalar ε into the state space representation of strictly proper plant G

$$\dot{x} = Ax + Bu \tag{17}$$

$$y = Cx + \varepsilon u \tag{18}$$

where A , B , and C are the system state matrix triple with $0 < \varepsilon \ll 1$. After ZOH discretization, the singular perturbed system is invertible using Eq. 7.

Similarly, we assume a chosen sampling frequency f_s such that the pole-zero pairs of singular perturbed system remain in the unit disc (Åström et al. 1984) and non-minimum phase behaviour of the plant is removed. formula in Eq. 7 can now be used with ε as a controller tuning parameter. When $0 < \varepsilon \ll 1$, we get the following approximation for true controlled output y

$$y \approx -Tn_1 - Sn_2 \tag{19}$$

We achieved almost disturbance suppression with simultaneous attenuation of noise sources n_1 and n_2 , not possible without additional sensor information.

4 Industrial application

In this section, we shall evaluate the effectiveness of the proposed DDO scheme for simplicity but without

loss of generality. Simulation and experiments are conducted on a PZT actuated head cartridge reported by Wong et al. (2005) and shown in Fig. 4.

It is worth noting that the PZT active suspension commonly envisaged for usage in future dual-stage HDDs can also be used. The nominal DDO is chosen to illustrate the effectiveness of our proposed schemes as it is well known from control theory that additional sensors improve servo performance if SNR (signal-to-noise ratio) and resolution of the sensors are satisfactory. Also, we expect the DDOS to perform better if extraneous sensors are available as the propositions and problem formulations for both DDO and DDOS are inherently similar.

The frequency response of the PZT actuated head cartridge with passive suspension is shown in Fig. 5. The nominal plant model of the PZT actuated head cartridge $G(s)$ is identified with resonant poles at 10.6 and 16.2 kHz as well as an anti-resonant zero at 13.8 kHz. For our application, the sway modes at these frequencies are identified while the torsional modes at 5.6 and 7.1 kHz are not included as they are out-of-plane (weakly uncontrollable). $G(s)$ is then discretized via a ZOH at a sampling rate f_s of 40 kHz so that the stable pole-zero pairs of $G(s)$ remain in the unit disc (Åström et al. 1984). The transfer function of the discretized plant $G(z)$ is identified as

$$G(z) = \frac{1.6919(z + 0.9729)(z^2 - 0.2433z + 0.8912)}{(z^2 - 0.854z + 0.9151)(z^2 + 0.2329z + 0.9033)} \tag{20}$$

The relative degree of the $G(z)$ is unity and hence Δ is set to zero.

For the digital controller $K(z)$, a practical integrator (by setting pole at 10 Hz instead of origin to prevent actuator saturation from very large low frequency gain) in series with a low pass filter of corner frequency

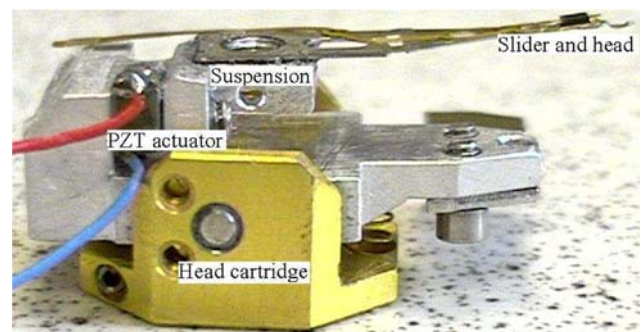


Fig. 4 PZT-actuated head cartridge with mounted passive suspension carrying a slider and R/W (read/write) head used in a spinstand

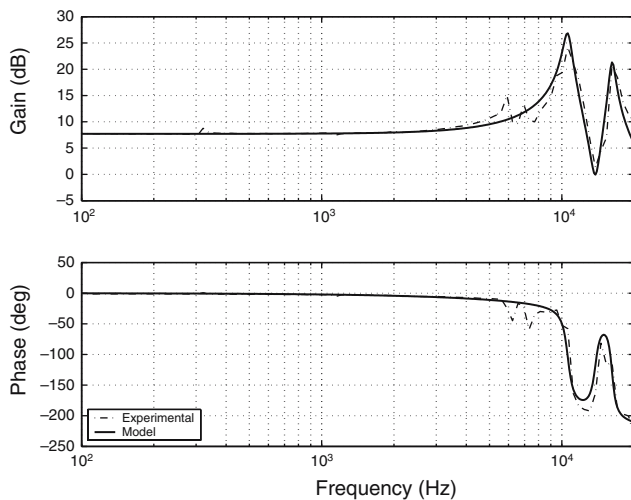


Fig. 5 Frequency response of the PZT actuated head cartridge with mounted passive suspension

at 5 kHz is used. An extra zero is placed near Nyquist frequency of 20 kHz to reduce the relative degree of $K(z)$ without affecting mid frequency performance, thereby achieving low sensitivity (Pang et al. 2005b). To tackle the resonant modes, digital notch filters are constructed to attenuate the large gains of the sway modes at 10.6 and 16.2 kHz caused by the PZT actuated passive suspension. As such, the transfer function of $K(z)$ considering the practical integrator, low pass filter, extra zero, notch filters and a gain to ensure the gain crossover frequency is at 3.5 kHz is given by

$$\begin{aligned}
 K(z) &= 0.033049 \\
 &\times \frac{z + 0.998z + 0.222z^2 + 1.623z + 0.9667}{z - 0.998z - 0.4361z^2 + 1.287z + 0.5597} \cdots \\
 &\times \frac{z^2 + 0.2405z + 0.9707}{z^2 + 0.1632z + 0.3367} \quad (21)
 \end{aligned}$$

The frequency response of $K(z)$ is shown in Fig. 6.

4.1 Simulation results

To illustrate the effectiveness of our proposed DDO, simulations are carried out with reference to a “standard” DO used for track following operations in HDD servo control as detailed by White et al. (2000). For the standard DO, the Q -filter is designed to be a second order transfer function of unity DC gain and damping with natural frequency at 3.5 kHz, corresponding to the gain crossover frequency of the nominal open loop transfer function. The plant inverse is design according to ZPET methodology detailed by White et al. (2000) and Tomizuka (1987).

4.1.1 Choice of ε

The performance of the proposed DDO is dependent on the accuracy of the plant inverse model \hat{G}^{-1} . The frequency response of $\hat{G}^{-1}(z)G(z)$ for different values of ε is shown in Fig. 7. From the above, it can be seen that decreasing ε effectively increases the frequency range where the $\hat{G}^{-1}(z)G(z) = 1$. However, further reduction of ε results in a larger peak at high frequencies which degrades closed-loop stability. Decreasing ε also increases the high frequency gain of the controller, resulting in amplification of measurement noise and high frequency signal amplification which might saturate the actuators. The authors recommend a range of $1 \times 10^{-4} \leq \varepsilon \leq 5 \times 10^{-3}$ for a compromise between performance of the DDO and noise attenuation. For the rest of our discussions, an $\varepsilon = 1 \times 10^{-3}$ is used.

4.1.2 Frequency responses

The simulated frequency responses of the open loop transfer functions without DO, with a standard DO and with our proposed DDO are shown in Fig. 8. The standard DO shapes the frequency response of the open loop transfer function at high frequencies (after gain crossover frequency) with increased phase lifting and reduced roll-off. The increased phase margin corresponds to a “lighter” servo system, increasing the phase margin for robust stability and reduces the seek time during short-span tracking operations. The reduced roll-off translates to a sensitivity transfer function with reduced positive area (or “hump”) after gain crossover frequency and hence impedes amplification of high frequency disturbances at frequencies where feedback control is degrading servo performance (Pang et al. 2005b).

With the proposed DDO, the low frequency gain is increased while maintaining the same gain crossover frequency at 3.5 kHz with alleviated phase delay and roll-off simultaneously as can be seen from Fig. 8. Due to parallel compensation, the open loop transfer function is able to achieve a higher bandwidth via the approximate plant inverse model \hat{G}^{-1} which compensates for the stable pole-zero pairs in plant G . The low frequency disturbance rejection performance is improved, coupled with an even lower positive area in sensitivity transfer function. This is verified with the simulated frequency responses of the sensitivity transfer functions S shown in Fig. 9. Stronger error rejection is achieved with the proposed DDO even though the

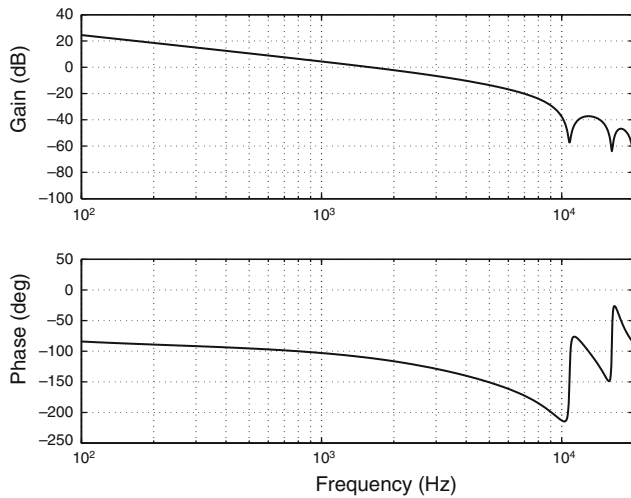


Fig. 6 Frequency response of designed controller $K(z)$

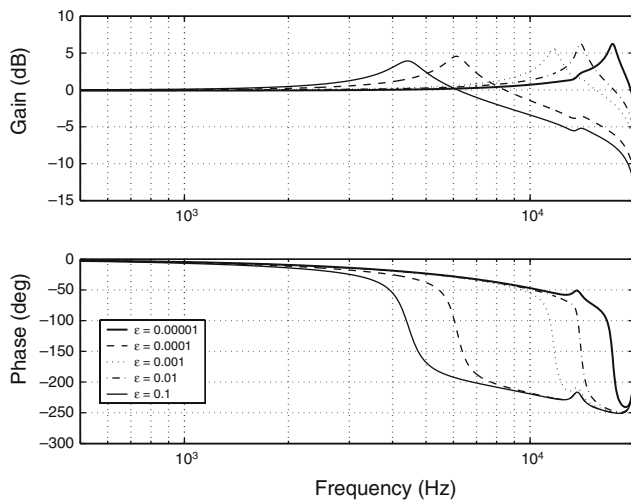


Fig. 7 Frequency response of $\hat{G}^{-1}(z)G(z)$ for different values of ϵ

gain crossover frequency is maintained at 3.5 kHz for all three cases.

The proposed DDO is linear and hence is still bounded by the “waterbed” effect as depicted by the Discrete Bode’s Integral Theorem (Mohtadi 1980). While much sensitivity reduction can be seen at most frequencies, the excavated sensitivity area at low frequencies and the “hump” is actually (and automatically) distributed evenly over high frequencies for low sensitivity up to Nyquist frequency i.e. the gain of the sensitivity transfer function reaches 0 dB more gradually but with a smaller amplitude. This phenomenon can be observed for the frequency responses of the sensitivity transfer functions of that with the standard DO and proposed DDO as shown in Fig. 9.

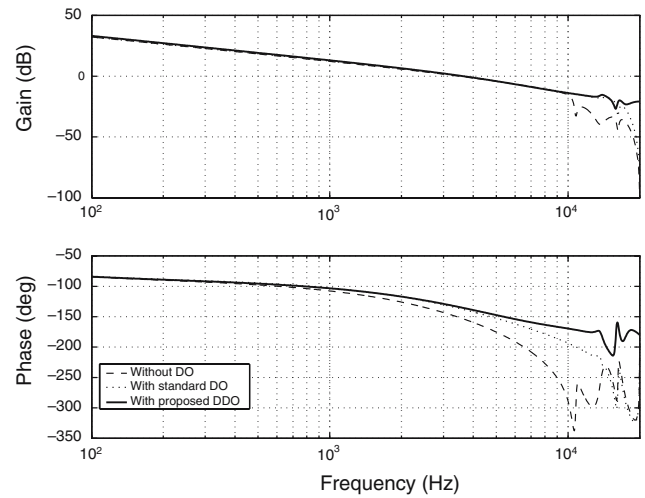


Fig. 8 Frequency responses of open loop transfer functions. Dashed without DO, dashed-dot with standard DO, solid with proposed DDO

4.1.3 PES test

To demonstrate the effectiveness of our proposed scheme, simulations are carried out to evaluate the 3σ PES or TMR (track mis-registration) during track following control operations where σ is the standard deviation. The identified vibration model and noise sources model reported by Du et al. (2002) with a Fujitsu fluid bearing spindle motor HDD rotating at 5,400 rpm is used to emulate output disturbances d_o and noise n , respectively. While the torque disturbance reported by Du et al. (2002) is not applicable, a low frequency sinusoid of $0.01 \sin(2\pi 50t) \mu\text{m}$ is used to simulate the effects of input disturbances d_i . The simulated measured PES e without DO, with a standard DO and with the proposed DDO are shown in Fig. 10. An improvement of 79.5% in 3σ PES e is observed.

The standard DO improves the 3σ PES from 0.0083 to 0.0074 μm (a 16.0% improvement) while the proposed DDO is able to reduce the 3σ PES further to 0.0017 μm , corresponding to a 79.5% improvement. The histograms of measured PES e without DO, with a standard DO and with the proposed DDO are shown in Fig. 11. The variance of PES e is greatly reduced.

4.1.4 Robustness analysis

For the algorithm to be used by data storage industries during mass production of HDDs, the performance of the proposed DDO should be robustly

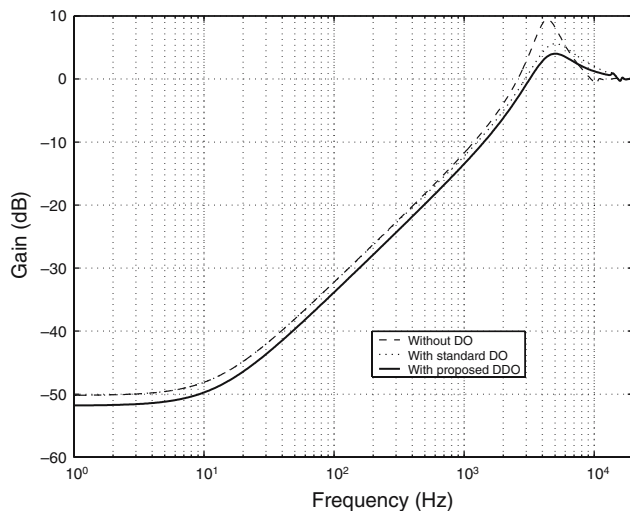


Fig. 9 Frequency responses of sensitivity transfer functions S . Dashed without DO, dashed-dot with standard DO, solid with proposed DDO

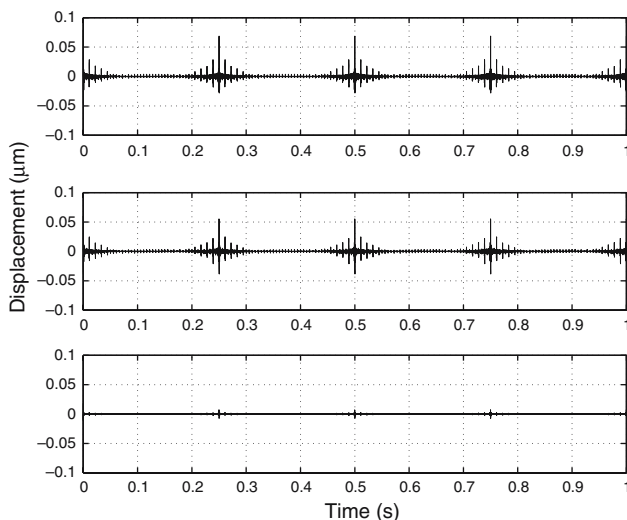


Fig. 10 Simulation results of measured PES e . Top without DO, middle with standard DO, bottom with proposed DDO

stable. To demonstrate the robustness of the proposed control scheme, we perturb the natural frequencies of the PZT actuated head cartridge with mounted passive suspension by up to $\pm 10\%$ as shown in Fig. 12.

The controller design for high bandwidth remains stable for the range of frequency uncertainties. However, degradation in percentage reduction of measured PES e occurs when the shift in resonant frequencies exceeds more than $\pm 7\%$ as can be seen in Fig. 13 although the nominal closed-loop remains robustly stable.

4.2 Experimental results

For our experiments, the LDV (Laser Doppler Vibrometer) is used as a displacement sensor to measure the displacement of the R/W head and the measured voltage output is collected as measured PES e .

4.2.1 Frequency responses

The experimental frequency response of open loop transfer function with the proposed DDO is shown in Fig. 14. The experimental frequency response of sensitivity transfer function S and complementary sensitivity transfer function T is drawn in Fig. 15.

From the figures above, it can be seen that experimental results tally well with the simulated frequency responses of open loop transfer function in Fig. 8 as well as sensitivity and complementary sensitivity transfer functions in Fig. 9.

4.2.2 Disturbance rejection test

In this section, we conduct experiments to showcase the effectiveness of the proposed control scheme in rejecting input disturbances d_i and output disturbances d_o simultaneously.

By closing the loop with $K(z)$ only and setting a zero reference, the measured PES e from the LDV and the corresponding control signal u is shown in Fig. 16. A low frequency measurement noise of about 20 Hz from the LDV is observed. The 3σ measured PES e is about $0.0174 \mu\text{m}$ for the length of data logged.

By including the proposed DDO with $K(z)$ and setting a zero reference, the measured PES e and the corresponding control signal u is shown in Fig. 17. The 3σ measured PES e is now about $0.0136 \mu\text{m}$ and hence a 16% improvement in 3σ measured PES e from 0.0174 to $0.0136 \mu\text{m}$ is obtained.

While the improvement seems trivial, we emulate a HDD environment using airflow with the centrifugal fan turned on as shown in Fig. 18. The windage across the entire passive suspension arm and air flow induced suspension vibrations are considered as input disturbances d_i and output disturbances d_o , respectively. The wind tunnel linearizes and concentrates the air flow and hence increases the airflow's mean speed to about 50 m/s, corresponding to the amount of airflow the R/W head experiences at the OD (outer diameter) of a 2.5" disk at a fast spindle rotation speed of 15,000 rpm in current high end server class HDDs. The air flow from the wind tunnel is directed at the entire passive

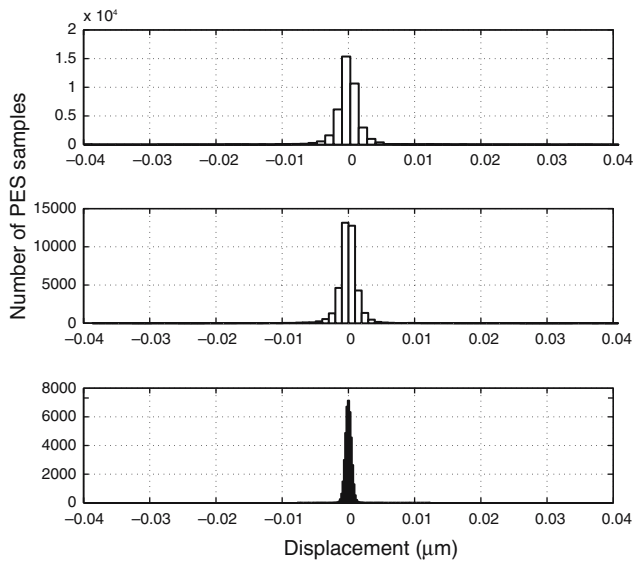


Fig. 11 Histogram of measured PES e . *Top* without DO, *middle* with standard DO, *bottom* with proposed DDO

suspension arm while the measure PES e is collected at the R/W head using the LDV.

With $K(z)$ only, the measured PES e and the corresponding control signal u is shown in Fig. 19. Although a high servo bandwidth of up to 3.5 kHz and low sensitivity controller are used, the amount of air flow on the passive suspension causes the R/W head to be deviated from the track centre on a large magnitude. The 3σ measured PES e now becomes

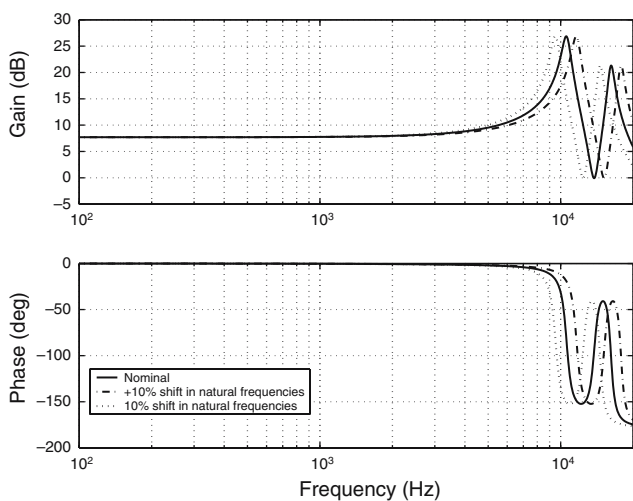


Fig. 12 Frequency responses of perturbed PZT-actuated head cartridge with mounted passive suspension by $\pm 10\%$

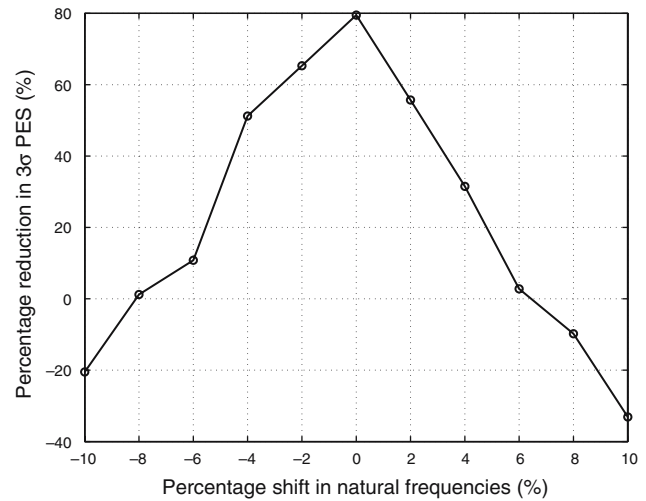


Fig. 13 Graph of 3σ PES versus percentage shift in resonant and anti-resonant frequencies

0.0578 μm with a horrendous deterioration of up to 230%.

By including the proposed DDO, the experiment is repeated with the centrifugal fan on. The measured PES e and the corresponding control signal u is shown in Fig. 20. The 3σ measured PES e is now about 0.0178 μm and hence a 69.2% improvement in 3σ measured PES e from 0.0578 to 0.0178 μm is observed. The DDO constricts the effects of input and output disturbances to bring the standard deviation of measured PES e near to the case without the centrifugal fan on.

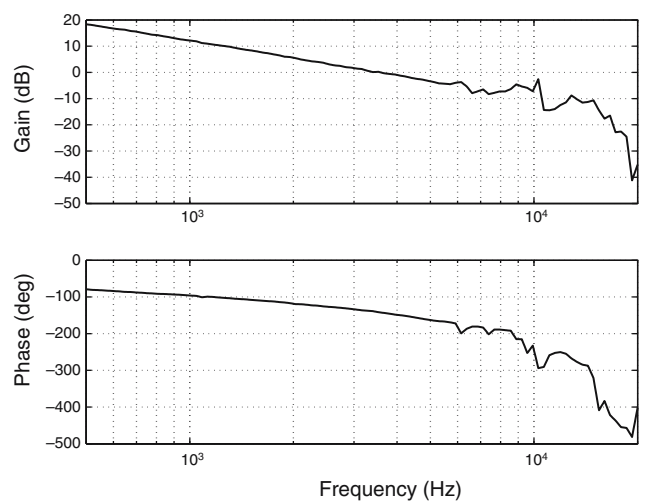


Fig. 14 Frequency response of experimental open loop transfer function with DDO

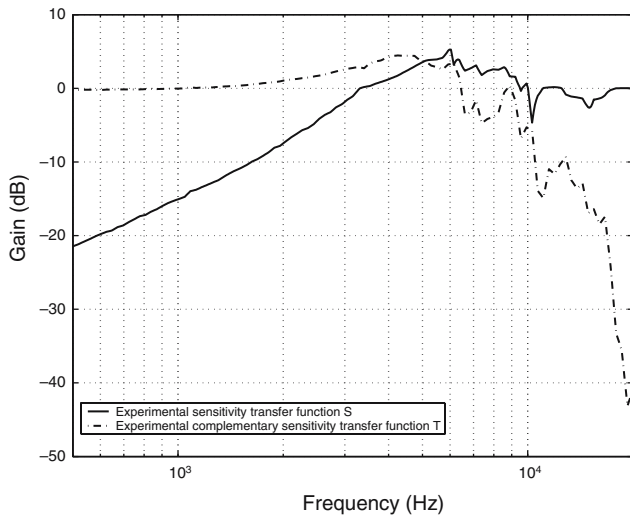


Fig. 15 Experimental frequency responses of sensitivity transfer functions with DDO

5 Conclusion

In this paper, a practical DDO and DDOS are proposed for stronger disturbance rejection in precise sampled-data servo systems. The proposed schemes are parameterized by a single parameter ϵ and are capable of rejecting input disturbances d_i and output disturbances d_o simultaneously, with possible simultaneous attenuation of noise sources from sensors with the DDOS. Experimental results on a PZT actuated head cartridge with mounted passive suspension for

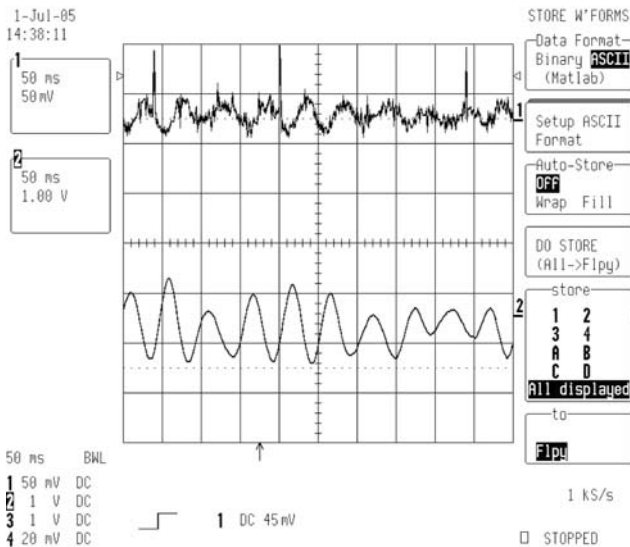


Fig. 16 Measured PES e in channel 1 (top) and control signal u in channel 2 (bottom) with nominal controller $K(z)$ only, i.e. without DDO

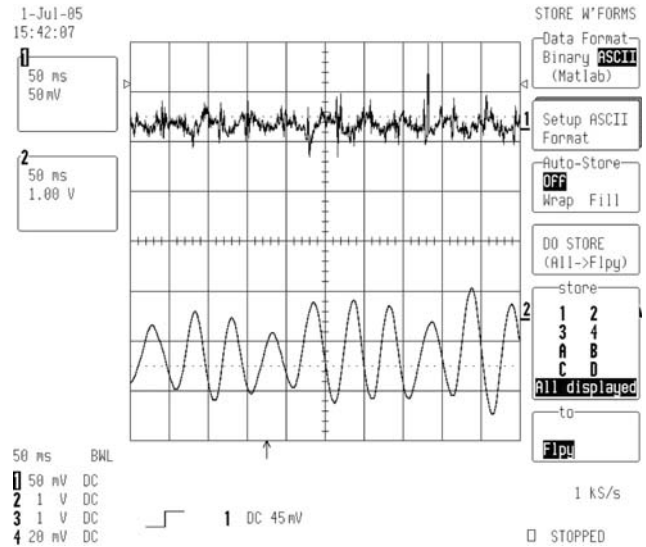


Fig. 17 Measured PES e in channel 1 (top) and control signal u in channel 2 (bottom) with controller $K(z)$ and proposed DDO

use in a servo spindown shows an improvement of 69.2% of 3σ PES during track-following when air flow of mean speed of 50 m/s corresponding to 15,000 rpm in today's high end HDDs mimicking input disturbances and output disturbances d_i and d_o , respectively, is blown on it. The proposed methodology can also be applied to probe-based storage systems or HDDs employing perpendicular recording technologies. Future works include applying the proposed DDO scheme as a noise differentiator to identify PES sensing noise model from measured PES e solely and implementing the DDOS using self-sensing to dual-stage HDDs.

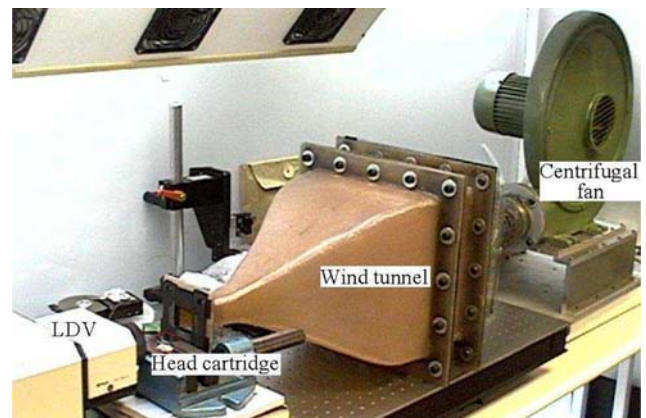


Fig. 18 Experiment setup showing LDV, PZT actuated passive suspension on head cartridge, a centrifugal fan and wind tunnel

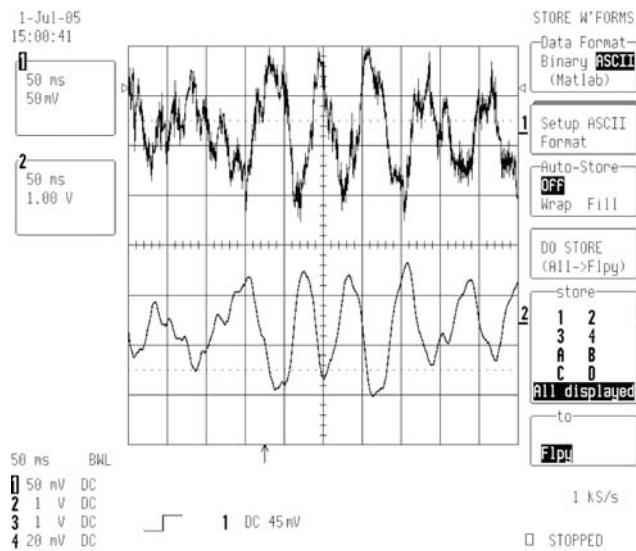


Fig. 19 Measured PES e in channel 1 (top) and control signal u in channel 2 (bottom) with controller $K(z)$ only, i.e. without DDO with the centrifugal fan on

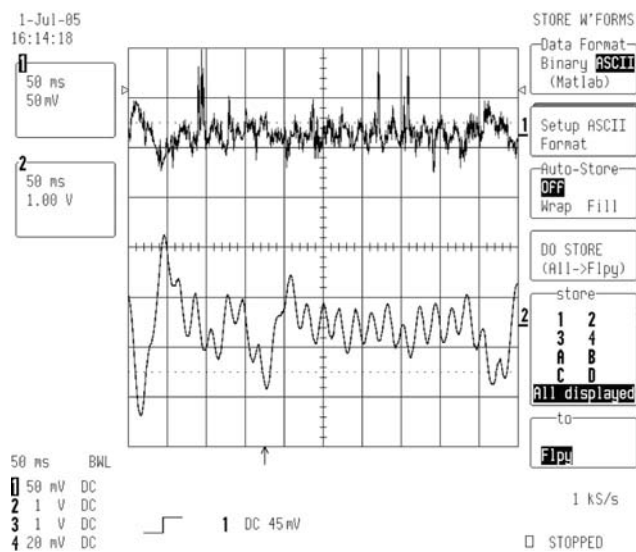


Fig. 20 Measured PES e in channel 1 (top) and control signal u in channel 2 (bottom) with controller $K(z)$ and proposed DDO with the centrifugal fan on

References

Åström KJ, Hagander P, Sternby J (1984) Zeros of sampled systems. *Automatica* 20(1):31–38

Chen BM, Lee TH, Hang CC, Guo Y, Weerasooriya S (1999) An H_∞ almost disturbance decoupling robust controller design for a piezoelectric bimorph actuator with hysteresis. *IEEE Trans Contr Syst Technol* 7(2):160–174

Du C, Zhang J, Guo G (2002) Vibration analysis and control design comparison of fluid bearing and ball bearing HDDs. In: *Proceedings of 2002 American Control Conference*, Anchorage, May 8–10, pp 1380–1385

Duan C (2005) Robust periodic disturbance compensation via multirate control. M. Eng. Thesis, National University of Singapore

Goodwin GC (2000) Predicting the performance of soft sensors as a route to low cost automation. *Ann Rev Control* 24:55–56

Kokotović PV, Khalil HK, O’Reilly J (1986) Singular perturbation methods in control: analysis and design. Academic, London

Lewis FL, Jagannathan S, Yeşildirek A (1999) Neural network control of robot manipulators and nonlinear systems. Taylor and Francis, London

Lin Z, Chen BM (2000) Solutions to general H_∞ almost disturbance decoupling problem with measurement feedback and internal stability for discrete-time systems. *Automatica* 36(8):1103–1122

Mohtadi C (1980) Bode’s integral theorem for discrete-time systems. *IEEE Proc* 137-D(2):57–66

Ohnishi K (1987) A new servo method in mechatronics. *Trans Jpn Soc Elect Eng* 107-D:83–86

Pang CK, Wong WE, Guo G, Chen BM, Lee TH (2005a) NRRO rejection using online iterative control for high density storage. *IEEE Trans Magn* (submitted)

Pang CK, Wu D, Guo G, Chong TC, Wang Y (2005b) Suppressing sensitivity hump in HDD dual-stage servo systems. *Microsyst Technol* 11(8–10):653–662

Pang CK, Guo G, Chen BM, Lee TH (2006) Self-sensing actuation for nanopositioning and active-mode damping in dual-stage HDDs. *IEEE/ASME Trans Mechatron* 11(3):328–338

Saberi A, Chen BM, Sannuti P (1993) Loop transfer recovery: analysis and design. Springer, London

Tomizuka M (1987) Zero phase error tracking algorithm for digital control. *J Dyn Syst Meas Control Trans ASME* 109:65–68

White MT, Tomizuka M, Smith C (2000) Improved track following in magnetic disk drives using a disturbance observer. *IEEE/ASME Trans Mechatron* 5(1):3–11

Wong WE, Feng L, He Z, Liu J, Kan CM, Guo G (2005) PC-based position error signal generation and servo system for a spindrive. *IEEE Trans Magn* 41(11):4315–4322